NANO LETTERS

Letter

pubs.acs.org/NanoLett

Negatively Charged Nitrogen-Vacancy Centers in a 5 nm Thin ^{12}C Diamond Film

K. Ohashi,[†] T. Rosskopf,[‡] H. Watanabe,[§] M. Loretz,[‡] Y. Tao,[‡] R. Hauert,[∥] S. Tomizawa,[†] T. Ishikawa,[†,⊥] J. Ishi-Hayase,[†] S. Shikata,[#] C. L. Degen,[‡] and K. M. Itoh*[,†]

[†]School of Fundamental Science and Technology, Keio University, Yokohama 223-8522, Japan

[‡]Department of Physics, ETH Zurich, Schafmattstrasse 16, 8093 Zurich, Switzerland

[§]Correlated Electronics Group, Electronics and Photonics Research Institute, National Institute of Advanced Industrial Science and Technology (AIST), Tsukuba Central 4, 1-1-1, Higashi, Tsukuba, Ibaraki 305-8562, Japan

[∥]Nanoscale Material Science, EMPA, Ueberlandstr. 129, 8600 Duebendorf, Switzerland

[⊥]Research Center for Advanced Science and Technology (RCAST), The University of Tokyo, Komaba, Meguro-ku, Tokyo 153-8904, Japan

[#]Diamond Research Group, Research Institute for Ubiquitous Energy Devices, National Institute of Advanced Industrial Science and Technology (AIST), 1-8-31, Midorigaoka, Ikeda, Osaka 563-8577, Japan

ABSTRACT: We report successful introduction of negatively charged nitrogen-vacancy (NV^-) centers in a 5 nm thin, isotopically enriched ($[^{12}C] = 99.99\%$) diamond layer by CVD. The present method allows for the formation of NV^- in such a thin layer even when the surface is terminated by hydrogen atoms. NV^- centers are found to have spin coherence times of between $T_2 \sim 10-100\ \mu s$ at room temperature. Changing the surface termination to oxygen or fluorine leads to a slight increase in the NV^- density, but not to any significant change in T_2. The minimum detectable magnetic field estimated by this T_2 is 3 nT after 100 s of averaging, which would be sufficient for the detection of nuclear magnetic fields exerted by a single proton. We demonstrate the suitability for nanoscale NMR by measuring the fluctuating field from $\sim 10^4$ proton nuclei placed on top of the 5 nm diamond film.

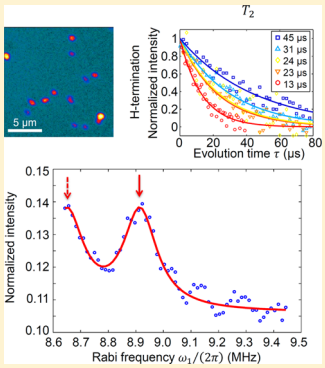

KEYWORDS: *Diamond, nitrogen-vacancy center, chemical vapor deposition, isotope engineering, magnetometry*

Since the experimental demonstrations of single electron- and nuclear-spin manipulation and readout,[1,2] the negatively charged nitrogen-vacancy (NV^-) center in diamonds has been considered one of the most promising solid-state qubits toward quantum information processing[3−7] and magnetometry.[8−14] Its spin properties are enhanced when placed in isotopically enriched ^{12}C diamonds leading to very long electron spin coherence times (~2 ms) at room temperature.[15,16]

There are two classes of magnetic field sensors based on NV centers in diamond: (i) two-dimensional (2D) imaging of the magnetic field distribution of the substance and/or structure by an ensemble of NV^-,[8,9] and (ii) detection of a small number of nuclear spins (ultimately a single nuclear spin) using a single NV^- center, preferably in a scanning probe arrangement.[10−12] The present paper focuses on the latter approach, which requires placement of single, isolated NV^- as close as possible to the surface of diamond. One of the ultimate goals in this scheme is the detection of single nuclear spins, which would allow performing nuclear magnetic resonance (NMR) investigations of single atoms and molecules placed on the diamond chip. Indeed, two groups have recently reported successful detection of a small ensemble of proton nuclear spins in an organic film placed on the surface of a bulk, single-crystal diamond using a single NV^- center.[17,18] Pushing this scheme to single nuclear spin detection requires formation of stable NV^- centers within a distance of <5 nm from the surface to provide sufficient dipolar coupling between the NV^- electron spin and a target nuclear spin.[10] Such small distances are also required to achieve a spatial resolution approaching the atomic level.[10] Realization of near-surface NV^- centers, however, faces the fundamental issue of limited charge stability due to so-called surface acceptor states. As depicted in Figure 1a, surface termination and adsorbate molecules can bend the band diagram upward near the surface and elevate the NV^- level above the Fermi level; that is, the NV centers near the surface prefer to take the neutral NV^0 states.[19−22] The NV^0 state is useless for the magnetic field sensing, since only NV^- exhibits the spin-dependent luminescence required to read out the NV spin state. The degree of surface bending was shown

Received: June 21, 2013
Revised: September 9, 2013

   dx.doi.org/10.1021/nl402286v | *Nano Lett.* XXXX, XXX, XXX−XXX

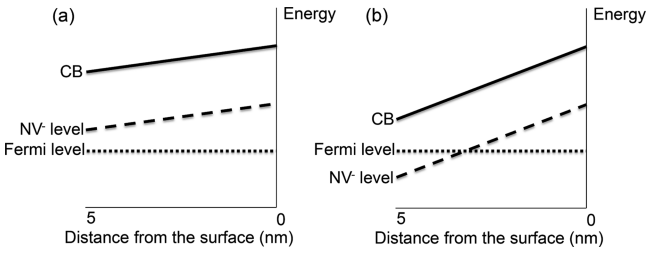

Figure 1. Schematics of the energy band bending near the surface. (a) For the case of low nitrogen concentration in the top 5 nm layer, the Fermi level remains far away from the conduction band (CB) and stays above the NV^- level to prohibit formation of the negatively charged NV centers. (b) When the nitrogen concentration in the top 5 nm film is large, the Fermi level is pushed closer to CB to situate partially above the NV^- level, allowing the NV centers here to become negatively charged.

theoretically and experimentally to depend on the kind of chemical species terminating the surface, among which the bending due to the hydrogen termination was the most pronounced.[19]

For magnetic field sensing the physical quantity directly connected to sensitivity is the coherence time T_2 of the electron bound to NV^-. The smallest ac magnetic field B_{min} detectable at optimal frequencies is given by,[23]

$$B_{\min} \sim \frac{\pi\hbar}{2g\mu_B C\sqrt{T_2 T}} \quad (1)$$

where g is the g-factor of the NV^- electron spin, μ_B is the Bohr magneton, T is the total measurement time, and C is a parameter related to experimental efficiency of collecting photons as defined in ref 23. Thus, a prospective NV^- placed near the surface must have long enough T_2 to achieve a B_{min} in the nanotesla regime.

A common approach employed in the past to produce near surface NV centers is to mill or synthesize diamond nanoparticles containing NV^-. These particles can have diameters down to 4–5 nm.[24−28] The longest T_2 recorded in these particles, however, are limited to a few microseconds at best,[24−26] falling far behind the values found for native defects in isotopically controlled single crystals ($T_2 \sim 2$ ms). On bulk single crystals, implantation of low energy nitrogen ions followed by appropriate annealing to form NV^- centers has been proven useful to a certain degree.[29−36] Although the distance of the NV centers from the surface can be approximately controlled by the appropriate selection of the ion acceleration energy and very shallow NV^- centers can be realized,[29] the depth distribution is statistically broadened, and it is impossible to know the exact depth of each single NV^- under observation. Moreover, the crystal damage associated with the implantation process may shorten T_2.

The goal of this study is to grow a heavily nitrogen doped, n+ top layer so as to suppress the band bending and stabilize NV^- centers very close to the surface (Figure 1b). While our recent work concentrated on the efficient introduction of well-behaved NV^- by nitrogen doping during the CVD growth of ∼100 nm thick, isotopically enriched ^{12}C films,[16] the present work performs band engineering at the surface to place NV^- having long enough T_2 for detection of single proton nuclear spins placed on the surface. We also note that our present approach is different from the method described in ref 37., where the nitrogen-doped layer was capped by a nominally undoped diamond layer.

An overview of our microwave plasma assisted chemical vapor deposition (MPCVD) method is described in detail elsewhere.[38] In the present study, MPCVD was performed using the microwave power of 750 W in the pressure of 25 Torr and the substrate temperature of 800 °C. A mixture of 0.5% isotopically enriched ($[^{12}C] = 99.99\%$) CH_4 and 99.5% H_2 was used as a feed gas. The substrate employed was a IIa (001) single crystal diamond grown by Sumitomo Electric Co. using a high-pressure and high-temperature (HPHT) method. The substrate is composed of the natural isotopic composition (∼98.9% ^{12}C and ∼1.1% ^{13}C, hereafter referred to as ^{nat}C) and reveals no trace of nitrogen when characterized by secondary ion mass spectroscopy (SIMS) and photoluminescence. On top of the substrate a 12-nm-thick ^{12}C buffer layer was grown by the above-mentioned condition. It has been confirmed that this condition does not introduce any NV centers in the film. On top of the buffer layer, a 5 nm thick heavily nitrogen doped layer was grown by adding natural nitrogen (^{nat}N) gas with the ratio $[^{nat}N/^{12}C] = 15\%$. Our previous work established that this ratio would lead to a nitrogen concentration $\sim 10^{18}$ cm^{-3} in the film.[39] The surface of as-grown CVD diamond is known to be terminated by hydrogen atoms (H-termination). The schematic of the structure is depicted in the inset of Figure 2a.

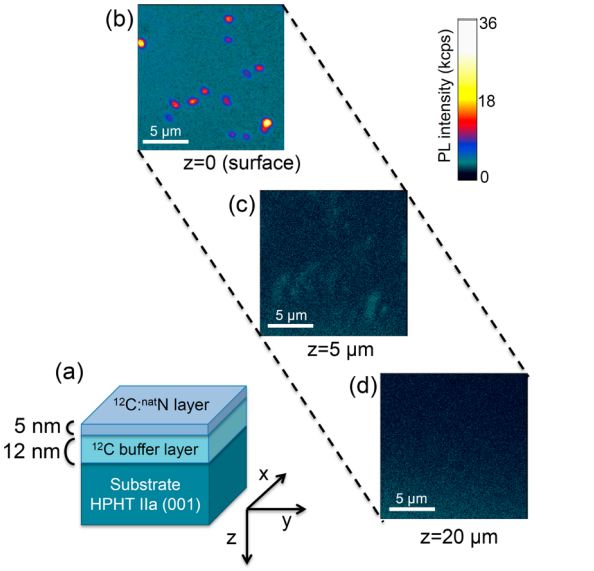

Figure 2. (a) A schematic of the diamond sample structure and (b–d) confocal photoluminescence (PL) scan images over the surface (XY) area of 16 × 16 μm^2 when the focus in the z-direction was placed at (b) ∼0 μm, (c) ∼5 μm, and (d) ∼20 μm from the surface of the top ^{12}C:^{nat}N layer. The depth resolution was approximately ∼0.5 μm. Emissions from single NV^- centers can been seen only in b.

Successful formation of NV^- centers in the 5 nm thick top layer was confirmed by scanning confocal photoluminescence (PL) measurement at room temperature. When the 532 nm excitation green laser was scanned over the sample surface (XY plane), PL having the characteristic spectrum in the 630–800 nm range appeared only from the surface region. This was confirmed by changing the focal point in the depth direction (Z direction) using a pinhole of 15 μm diameter. Although the resolution in Z-direction is rather coarse (∼0.5 μm), Figure 2b–d shows that there is very little emission from the substrate

dx.doi.org/10.1021/nl402286v | Nano Lett. XXXX, XXX, XXX–XXX

region, as expected. In fact, no single NV center could be found in the substrate over the entire course of this study, and our recently study, which will be written up elsewhere, has shown that all NV^- are contained in the depth between 2 and 5 nm from the surface. Here, the *XY* scan in a 16 × 16 μm^2 region was repeated three times to obtain PL from the depth of ~0 μm, ~5 μm, and ~20 μm. The surface density of the bright spots in the surface region (Figure 2b) was found to be (1.6 ± 0.5) × 10^5 cm^{-2}, which corresponds to a bulk density of ~3 × 10^{11} cm^{-3} assuming a thickness of 5 nm. To confirm that the bright spots correspond to NV^- centers, the PL spectrum from a variety of single spot was analyzed at room temperature. A typical spectrum obtained is shown in Figure 3a. Two diamond

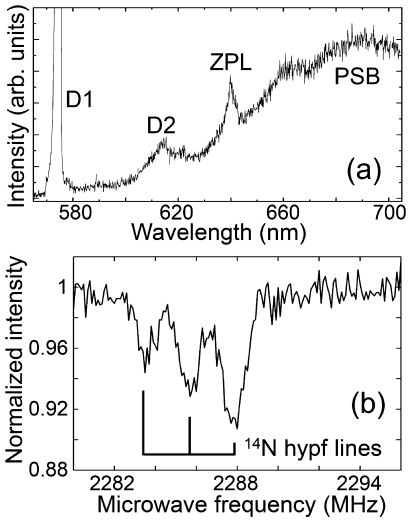

Figure 3. (a) A typical PL spectrum from a bright spot in Figure 2b recorded at room temperature. A zero phonon line (ZPL) and a phonon sideband (PSB) of NV^- centers appear clearly. D1 and D2 are the Raman peaks of diamonds. (b) Optically detected magnetic resonance (ODMR) of a typical single spot recorded at room temperature with the magnetic field 20 mT applied in a ⟨111⟩ direction. Three hyperfine (hypf) lines due to coupling to a ^{14}N (I = 1) isotope are clearly distinguishable.

Raman peaks (D1 and D2), the zero phonon line (ZPL) of NV^-, and the associated phonon sideband (PSB) are clearly visible. In addition, we performed optically detected magnetic resonance (ODMR) measurements of these bright spots to show conclusively that the emission arises from NV^-. Figure 3b shows a high-resolution ODMR scan recorded with a magnetic field of 20 mT applied along the ⟨111⟩ direction.[40] Here a hyperfine splitting of the NV^- electron spin states is clearly visible due to coupling to the ^{14}N (I = 1) nuclear spin. Similar spectra were recorded from all of the other stable bright spots. This confirms the successful formation of NV^- centers in the 5 nm thin layer.

To further characterize the spin properties of these NV^- centers a series of spin lifetime measurements was performed. In particular, the spin dephasing time T_2* (Ramsey measurement), the spin coherence time T_2 (spin echo measurement), and the longitudinal relaxation time T_1 were determined. All of the measurements were performed at room temperature with a magnetic field of ~7 mT in the ⟨111⟩ direction. The decay times were derived from exponential fits to the measured decay curves (Figure 4). The measurements yielded T_2* between 710 and 810 ns (data not shown), T_2 between 13 and 45 μs, and T_1

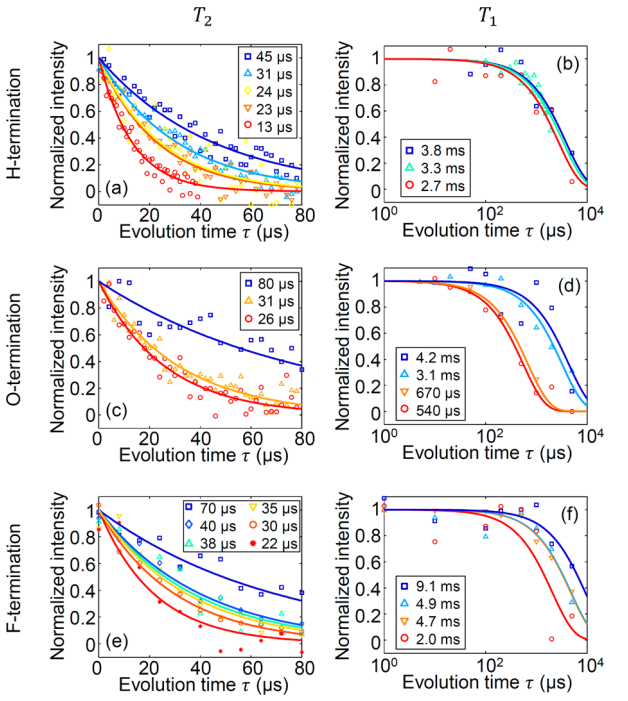

Figure 4. Room temperature spin echo and spin relaxation measurements of several NV centers with different surface terminations. For the hydrogen-terminated case, (a) room temperature spin echo in the 5 nm thin ^{12}C film showing T_2 ~ 13−45 μs. (b) room temperature spin relaxation showing T_1 ~ 2.7−3.8 ms. For the oxygen terminated case, (c) spin echo showing T_2 ~ 26−80 μs. (d) Room temperature spin relaxation showing T_1 ~ 0.54−4.2 ms. For the fluorine terminated case, (e) spin echo showing T_2 ~ 22−70 μs. (d) Room temperature spin relaxation showing T_1 ~ 2.0−9.1 ms.

between 2.7 and 3.8 ms. Note the absence of the electron spin echo envelope modulation (ESEEM)[41] in measurements of the spin echo decay (Figure 4a), which is characteristic of NV^- electron spins embedded in a ^{13}C nuclear spin free environment.[42,43] This observation confirms that the NV^- under observation is indeed located in the ^{12}C film and not in the underlaying ^{nat}C substrate. We note that the average value of the coherence time T_2 = 27 ± 11 μs, determined from five different NV^- centers, is much shorter than T_2 ~ 1.8 ms reported for NV^- in isotopically enriched ^{12}C diamonds and also in epitaxially overgrown N-doped diamond.[15,16,37] We suspect that both the high concentration (~10^{18} cm^{-3}) of nitrogen and the presence of magnetic surface states contribute to the shortening of T_2 in our 5 nm thick film. Whether it is possible to reduce the nitrogen concentration without affecting charge NV^- stability or replacing nitrogen by other donors will be the subject of future studies. We shall, however, stress again that introduction of a high concentration of nitrogen donors was key to our successful formation of NV^- near the surface, and we show below that our T_2 are still long enough for a possible single proton nuclear spin detection experiment.

We shall now discuss the effect of chemical surface termination on shallow NV^- centers. It has been shown previously that the unfavorable band bending in the hydrogen-terminated diamond is reduced significantly when the surface was terminated by other chemical species, such as oxygen.[20,21] Thus, a change of surface termination should enhance the formation of the negatively charged NV^- states near the surface.

dx.doi.org/10.1021/nl402286v | *Nano Lett.* XXXX, XXX, XXX−XXX

Table 1. Comparison of T_2, T_1, and T_2* of the NV^- Electrons at Room Temperature between Various Diamond Samples

type	sample	surface termination	distance from surface d (nm) or particle size φ (nm)	T_2 (μs)	T_1 (ms)	T_2* (ns)
CVD	this work	hydrogen	$d < 5$	45	3.8	810
	this work	oxygen	$d < 5$	80	4.2	980
	this work	fluorine	$d < 5$	70	9.1	
	Ohno et al.[37]	oxygen	$d = 5$	187		
	Ohno et al.[18,37]	oxygen	$d = 21$	606		
	Ohno et al.[37]	oxygen	$d = 52$	765		
	Ohno et al.[37]	oxygen	$d = 103$	800		
	Ishikawa et al.[16]	hydrogen	$d < 100$	1700		90000
ion implanation	Ofori-Okai et al.[29]	oxygen	$d = 1.1 \pm 0.6$	12.2		
	Ofori-Okai et al.[29]	oxygen	$d = 7.7 \pm 3.1$	40.4		
	Staudacher et al.[35]	oxygen	$d = 5 \pm 5$	6.2	1.8	
	Staudacher et al.[35]		$d = 35 \pm 5$	171.1	3.1	
	Maletinsky et al.[36]		$d = 10 \pm 10$	74.8		
nanoparticle	Tisler et al.[24]	oxygen	$\varphi = 7$	1.4		
	Boudou et al.[25]	oxygen	$\varphi = 7$	2.7		
	Boudou et al.[25]	oxygen	$\varphi = 15$	1.9		
	Maze et al.[12]		$\varphi = 30$	4		
	Laraoui et al.[26]		$\varphi = 45$	3.2		238

We have investigated the same diamond sample after the surface was terminated by oxygen and fluorine, respectively. To realize oxygen-termination (O-termination), the sample was boiled in a mixture of sulphuric, nitric, and perchloric acids (volume ratio 1:1:1) at 92 °C for 16 h.[24] For fluorine-termination (F-termination), the sample was briefly (15 s) exposed to CF_4 plasma.[44] A water contact angle measurement was used to confirm the change in the surface energy between H- and O-termination. XPS measurements were carried out to confirm the complete replacement of atomic species between O- and F-termination.

Photoluminescence measurements of the surface reveal an NV^- density of $(2.2 \pm 0.6) \times 10^5$ cm^{-2} for O-termination and $(6.2 \pm 1.2) \times 10^5$ cm for F-termination, which is slightly higher than $(1.6 \pm 0.5) \times 10^5$ cm^{-2} for the H-terminated surface, confirming observations of earlier measurements on deeper NV^- centers.[20,45,46] Interestingly, for F-termination, a significant fraction of identified NV centers (roughly 30%) bleached during the course of investigation after a few hours of exposure to laser illumination. No bleaching was observed under H- or O-termination. We suspect that the F-termination either exerts a positive charge on the underlying surface or favors stable charge traps on the surface, promoting ionization to the neutral NV^0 charge state.

We found T_2 values to not change significantly between surface terminations, as shown in Figure 4c,e. We suspect that T_2 is mainly limited by the high nitrogen doping concentration, and hence there is little influence of surface chemistry. Longitudinal relaxation times T_1, on the other hand, show a much larger spread especially for O-termination. Here, it may be possible that the O-termination stabilizes NV^- centers closer to the surface. NV centers situated closer to the surface should have shorter T_1 due to coupling to magnetic defects at the surface, leading to a larger variation in T_1.[47] Table 1 summarizes the results of the present study along with those reported recently for various diamond samples containing NV^- close to surfaces. Here three different groups of samples—CVD diamond films with in situ nitrogen doping during growth, bulk diamond samples with nitrogen doping by ion implantation, and nanoparticles prepared by a various methods—are listed. Only in the present study coherence times of NV^- were obtained for the three different surface terminations; hydrogen, oxygen, and fluorine. Also, both T_2 and T_1 are longer for NV^- formed in the CVD films compared to those formed by ion implantation and situated at the same distance from the surface.

Finally, we have explored the suitability of the NV^- created in our present 5 nm diamond film for detecting small ensembles and ultimately a single proton nuclear spin. To establish whether a proton signal can be detected, we have overcoated the sample with immersion oil that has a high hydrogen content of $\sim 6 \times 10^{22}$ cm^{-3}.[48] Figure 5 shows a spectrum of magnetic fluctuations between 8.7 and 9.4 MHz, recorded in a magnetic bias field of 210 mT using the spin-locking magnetic sensing protocol.[13] A peak at 8.915 MHz is clearly seen, identifying the proton nuclear spin species that has a Larmor frequency of 42.57 MHz/T. From the magnitude of the signal ($B_{rms} \sim 0.8$ μT) and the proton density we deduce that the depth of this NV center is approximately 5.1 nm and that on the order of 10^3–10^4 statistically polarized protons

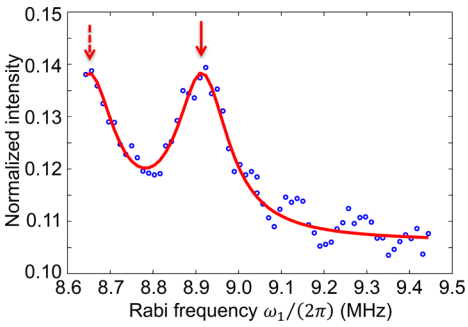

Figure 5. Example of detection of a small ensemble of proton spins on top of the present 5 nm diamond film, showing the suitability for nuclear spin sensing. The main proton peak at 8.915 MHz is indicated by a red arrow. Blue dots are experimental data, and the red curve is a calculation using an rms-magnetic field of 780 nT and a line width of 140 kHz. The magnetic bias field is 210 mT, and the evolution time is 50 μs. The second peak at 8.650 MHz (dashed arrow) is a replica of the main peak due to the hyperfine structure introduced by the ^{14}N nuclear spin.[13] The broad NMR line width is much larger than the detection bandwidth (~20 kHz) and probably due to rapid diffusion of molecules through the nanometer detection volume.

dx.doi.org/10.1021/nl402286v | Nano Lett. XXXX, XXX, XXX–XXX

contribute to the signal.[13,17] This proves the suitability of our controlled 5 nm thin film sample for nanoscale NMR applications. One should however note that the line width ~140 kHz of the proton NMR peak is larger than that of ~14 kHz observed in ref 17. This may be due to the different immersion oils, that is, different samples, employed in the measurements. For example, our oil had a higher proton content than the one employed in ref 17, and other characteristics (e.g., compositions, viscosity, etc.) are likely also different.

Let us now discuss the outlook of detecting a single proton nuclear spin. The magnetic field B_{proton} at a NV arising from a single proton at distance r away is given by

$$B_{proton} \sim \frac{\mu_0}{4\pi}\frac{3\cos^2\theta - 1}{r^3}\mu_p \quad (2)$$

where μ_0 is the vacuum permeability, $\mu_p = 1.41 \times 10^{-26}$ J/T is the magnetic dipole moment of the proton, and θ is the angle between the proton and electron spin precession axes. Thus the magnetic field at the distance $r = 5$ nm away from the proton is ~11 nT. Using eq 1 with $T_2 \sim 45$ μs, $C \sim 0.05$, and a total measurement time of $T = 100$ s,[12,23] the smallest detectable ac magnetic field becomes $B_{min} \sim 3$ nT. This would be sufficient to detect the 11 nT field of a single proton spin with the signal-to-noise ratio of about 3.

In conclusion, we have succeeded in the formation of isolated NV^- centers within a 5 nm thin, ^{12}C-isotopically enriched diamond layer by heavy nitrogen doping during microwave plasma assisted chemical vapor deposition, even for a hydrogen-terminated surface. We believe that the high concentration of nitrogen donors suppresses band bending near the surface and stabilizes negatively charged NV centers near the surface. Measured NV^- centers exhibit dephasing times $T_2^* = 0.71-0.81$ μs, coherence times $T_2 = 13-45$ μs, and spin−lattice relaxation times T_1~2.7−3.8 ms at room temperature. The change of the surface chemistry to oxygen and fluorine termination yielded a slight increase in NV^- density with no significant change in T_2. Coherence times found are sufficiently long to detect a small ensemble of nuclear spins on the surface of diamond and, if individual protons can be well isolated, can provide the magnetic sensitivity needed for single nuclear spin detection.

AUTHOR INFORMATION

Corresponding Author

*E-mail: kitoh@appi.keio.ac.jp.

Notes

The authors declare no competing financial interest.

ACKNOWLEDGMENTS

We thank fruitful discussions with K. M. Fu, C. Santori, V. M. Acosta, K. Fang, H. Umezawa, and R. G. Beausoleil. The work at Keio has been supported in part by Cannon Foundation, in part by NEXT, in part by the Core-to-Core Program by JSPS, and in part by the Project for Developing Innovation Systems by MEXT. The work at ETH has been supported by the Swiss National Science Foundation through grant 200021_137520/1 and through the NCCR QSIT.

REFERENCES

(1) Gruber, A.; Dräbenstedt, A.; Tietz, C.; Fleury, L.; Wrachtrup, J.; von Borczyskowski, C. *Science* **1997**, *272*, 2012.
(2) Jelezko, F.; Gaebel, T.; Popa, I.; Gruber, A.; Wrachtrup, J. *Phys. Rev. Lett.* **2004**, *92*, 076401.
(3) Santori, C.; Tamarat, P.; Neumann, P.; Wrachtrup, J.; Fattal, D.; Beausoleil, R. G.; Rabeau, J.; Olivero, P.; Greentree, A. D.; Prawer, S.; Jelezko, F.; Hemmer, P. *Phys. Rev. Lett.* **2006**, *97*, 247401.
(4) Togan, E.; Chu, Y.; Trifonov, A. S.; Jiang, L.; Maze, J.; Childress, L.; Dutt, M. V. G.; Sorensen, A. S.; Hemmer, P. R.; Zibrov, A. S.; Lukin, M. D. *Nature (London)* **2010**, *466*, 730.
(5) Kubo, Y.; Ong, F. R.; Bertet, P.; Vion, D.; Jacques, V.; Zheng, D.; Dreau, A.; Roch, J.-F.; Auffeves, A.; Jelezko, F.; Wrachtrup, J.; Barthe, M. F.; Bergonzo, P.; Esteve, D. *Phys. Rev. Lett.* **2010**, *105*, 140502.
(6) Fuchs, G. D.; Burkard, G.; Klimov, P. V.; Awschalom, D. D. *Nat. Phys.* **2011**, *7*, 790.
(7) Zhu, X.; Saito, S.; Kemp, A.; Kakuyanagi, K.; Karimoto, S.; Nakano, H.; Munro, W. J.; Tokura, Y.; Everitt, M. S.; Nemoto, K.; Kasu, M.; Mizuochi, N.; Semba, K. *Nature (London)* **2011**, *478*, 221.
(8) Pham, L. M.; Le Sage, D.; Stanwix, P. L.; Yeung, T. K.; Glenn, D.; Trifonov, A.; Cappellaro, P.; Hemmer, P. R.; Lukin, M. D.; Park, H.; Yacoby, A.; Walsworth, R. L. *New J. Phys.* **2011**, *13*, 045021.
(9) Hall, L. T.; Beart, G. C. G.; Thomas, E. A.; Simpson, D. A.; McGuinness, L. P.; Cole, J. H.; Manton, J. H.; Scholten, R. E.; Jelezko, F.; Wrachtrup, J.; Petrou, S.; Hollenberg, L. C. L. *Sci. Rep.* **2012**, *2*, 401.
(10) Degen, C. L. *Appl. Phys. Lett.* **2008**, *92*, 243111.
(11) Balasubramanian, G.; Chan, I. Y.; Kolesov, R.; Al-Hmoud, M.; Tisler, J.; Shin, C.; Kim, C.; Wojcik, A.; Hemmer, P. R.; Krueger, A.; Hanke, T.; Leitenstorfer, A.; Bratschitsch, R.; Jelezko, F.; Wrachtrup, J. *Nature (London)* **2008**, *455*, 648.
(12) Maze, J. R.; Stanwix, P. L.; Hodges, J. S.; Hong, S.; Taylor, J. M.; Cappellaro, P.; Jiang, L.; Dutt, M. V. G.; Togan, E.; Zibrov, A. S.; Yacoby, A.; Walsworth, R. L.; Lukin, M. D. *Nature (London)* **2008**, *455*, 644.
(13) Loretz, M.; Rosskopf, T.; Degen, C. L. *Phys. Rev. Lett.* **2013**, *110*, 017602.
(14) Fang, K.; Acosta, V. M.; Santori, C.; Huang, Z.; Itoh, K. M.; Watanabe, H.; Shikata, S.; Beausoleil, R. G. *Phys. Rev. Lett.* **2013**, *110*, 130802.
(15) Balasubramanian, G.; Neumann, P.; Twitchen, D.; Markham, M.; Kolesov, R.; Mizuochi, N.; Isoya, J.; Achard, J.; Beck, J.; Tissler, J.; Jacques, V.; Hemmer, P. R.; Jelezko, F.; Wrachtrup, J. *Nat. Mater.* **2009**, *8*, 383.
(16) Ishikawa, T.; Fu, K. M.; Santori, C.; Acosta, V. M.; Beausoleil, R. G.; Watanabe, H.; Shikata, S.; Itoh, K. M. *Nano Lett.* **2012**, *12*, 2083.
(17) Staudacher, T.; Shi, F.; Pezzagna, S.; Meijer, J.; Du, J.; Meriles, C. A.; Reinhard, F.; Wrachtrup, J. *Science* **2013**, *339*, 561.
(18) Mamin, H. J.; Kim, M.; Sherwood, M. H.; Rettner, C. T.; Ohno, K.; Awschalom, D. D.; Rugar, D. *Science* **2013**, *339*, 557.
(19) Grotz, B.; Hauf, M. V.; Dankerl, M.; Naydenov, B.; Pezzagna, S.; Meijer, J.; Jelezko, F.; Wrachtrup, J.; Stutzmann, M.; Reinhard, F.; Garrido, J. A. *Nat. Commun.* **2012**, *3*, 729.
(20) Hauf, V. M.; Grotz, B.; Naydenov, B.; Dankerl, M.; Pezzagna, S.; Meijer, J.; Jelezko, F.; Wrachtrup, J.; Stutzmann, M.; Reinhard, F.; Garrido, J. A. *Phys. Rev. B* **2011**, *83*, 081304(R).
(21) Fu, K. M. C.; Santori, C.; Barclay, P. E.; Beausoleil, R. G. *Appl. Phys. Lett.* **2010**, *96*, 121907.
(22) Petrakova, V.; Nesladek, M.; Taylor, A.; Fendrych, F.; Cigler, P.; Ledvina, M.; Vacik, J.; Stursa, J.; Kucka, J. *Phys. Status Solidi A* **2011**, *208*, 2051.
(23) Taylor, J. M.; Cappellaro, P.; Childress, L.; Jiang, L.; Budker, D.; Hemmer, P. R.; Yacoby, A.; Walsworth, R.; Lukin, M. D. *Nat. Phys.* **2008**, *4*, 810.
(24) Tisler, J.; Balasubramanian, G.; Naydenov, B.; Kolesov, R.; Grotz, B.; Reuter, R.; Boudou, J.; Curmi, P. A.; Sennour, M.; Thorel, A.; Borsch, M.; Aulenbacher, K.; Erdmann, R.; Hemmer, P. R.; Jelezko, F.; Wrachtrup, J. *ACS Nano* **2009**, *3*, 1959.
(25) Boudou, J.-P.; Tisler, J.; Reuter, R.; Thorel, A.; Curmi, P. A.; Jelezko, F.; Wrachtrup, J. *Diamond Relat. Mater.* **2013**, *37*, 80.
(26) Laraoui, A.; Hodges, J. S.; Meriles, C. A. *Nano Lett.* **2012**, *12*, 3477.

(27) Sonnefraud, Y.; Cuche, A.; Faklaris, O.; Boudou, J.; Sauvage, T.; Roch, J.; Treussart, F.; Huant, S. *Opt. Lett.* **2008**, *33*, 611.
(28) Smith, B. R.; Inglis, D. W.; Sandnes, B.; Rabeau, J. R.; Zvyagin, A. V.; Gruber, D.; Noble, C. J.; Vogel, R.; Osawa, E.; Plakhotnik, T. *Small* **2009**, *5*, 1649.
(29) Ofori-Okai, B. K.; Pezzagna, S.; Chang, K.; Schirhagl, R.; Tao, Y.; Moores, B. A.; Groot-Berning, K.; Meijer, J.; Degen, C. L. *Phys. Rev. B* **2012**, *86*, 081406(R).
(30) Aharonovich, I.; Santori, C.; Fairchild, B. A.; Orwa, J.; Ganesan, K.; Fu, K. M.; Beausoleil, R. G.; Greentree, A. D.; Prawer, S. J. *Appl. Phys.* **2009**, *106*, 124904.
(31) Toyli, D. M.; Weis, C. D.; Fuchs, G. D.; Schenkel, T.; Awschalom, D. D. *Nano Lett.* **2010**, *10*, 3168.
(32) Naydenov, B.; Reinhard, F.; Lämmle, A.; Richter, V.; Kalish, R.; D'Haenens-Johansson, U. F. S.; Newton, M.; Jelezko, F.; Wrachtrup, J. *Appl. Phys. Lett.* **2010**, *97*, 242511.
(33) Pezzagna, S.; Naydenov, B.; Jelezko, F.; Wrachtrup, J.; Meijer, J. *New J. Phys.* **2010**, *12*, 065017.
(34) Orwa, J. O.; Santori, C.; Fu, K. M. C.; Gibson, B.; Simpson, D.; Aharonovich, I.; Stacey, A.; Cimmino, A.; Balog, P.; Markham, M.; Twitchen, D.; Greentree, A. D.; Beausoleil, R. G.; Prawer, S. J. *Appl. Phys.* **2011**, *109*, 083530.
(35) Staudacher, T.; Ziem, F.; Häussler, L.; Stöhr, R.; Steinert, S.; Reinhard, F.; Scharpf, J.; Denisenko, A.; Wrachtrup, J. *Appl. Phys. Lett.* **2012**, *101*, 212401.
(36) Maletinsky, P.; Hong, S.; Grinolds, M. S.; Hausmann, B.; Lukin, M. D.; Walsworth, R. L.; Loncar, M.; Yacoby, A. *Nat. Nanotechnol.* **2012**, *7*, 320.
(37) Ohno, K.; Heremans, F. J.; Bassett, L. C.; Myers, B. A.; Toyli, D. M.; Bleszynski Jayich, A. C.; Palmstrøm, C. J.; Awschalom, D. D. *Appl. Phys. Lett.* **2012**, *101*, 082413.
(38) Watanabe, H.; Takeuchi, D.; Yamanaka, S.; Okushi, H.; Kajimura, K.; Sekiguchi, T. *Diamond Relat. Mater.* **1999**, *8*, 1272.
(39) Watanabe, H.; Kitamura, T.; Nakashima, S.; Shikata, S. *J. Appl. Phys.* **2009**, *105*, 093529.
(40) Dreau, A.; Lesik, M.; Rondin, L.; Spinicelli, P.; Arcizet, O.; Roch, J. F.; Jacques, V. *Phys. Rev. B* **2011**, *84*, 195204.
(41) Mims, W. B. *Phys. Rev. B* **1972**, *5*, 2409. Mims, W. B. *Phys. Rev. B* **1972**, *6*, 3543.
(42) Oort, E. V.; Glasbeek, M. *Chem. Phys.* **1990**, *143*, 131.
(43) Childress, L.; Dutt, M. V. G.; Taylor, J. M.; Zibrov, A. S.; Jelezko, F.; Wrachtrup, J.; Hemmer, P. R.; Lukin, M. D. *Science* **2006**, *314*, 281.
(44) Schvartzman, M.; Wind, S. J. *Nanotechnology* **2009**, *20*, 145306.
(45) Cui, S.; Hu, E. L. *Appl. Phys. Lett.* **2013**, *103*, 051603.
(46) Petráková, V. *Acta Polytech.* **2011**, *51* (No. 5), 89.
(47) Tetienne, J.-P.; Hingant, T.; Rondin, L.; Cavaill, A.; Mayer, L.; Dantelle, G.; Gacoin, T.; Wrachtrup, J.; Roch, J.-F.; Jacques, V. *arXiv*, 1304.1197.
(48) The proton content of the oil was measured by mass spectrometry.